Earth and Planetary Science Letters 275 (2008) 111–120

Contents lists available at ScienceDirect

Earth and Planetary Science Letters

journal homepage: www.elsevier.com/locate/epsl

(U–Th)/He dating of kimberlites—A case study from north-eastern Kansas

Terrence J. Blackburn [a,*], Daniel F. Stockli [a], Richard W. Carlson [b], Pieter Berendsen [c]

[a] University of Kansas Department of Geology, 1475 Jayhawk Blvd Rm 120, Lawrence, KS 66044, USA
[b] Department of Terrestrial Magnetism, Carnegie Institution of Washington 5241 Broad Branch Road, NW Washington, DC 20015-1305, USA
[c] Kansas Geological Survey, 1930 Constant Ave., Lawrence, KS 66047-3726, USA

ARTICLE INFO

Article history:
Received 9 January 2008
Received in revised form 5 August 2008
Accepted 7 August 2008
Available online 26 September 2008

Editor: M.L. Delaney

Keywords:
(U–Th)/He
Rb–Sr
kimberlite
Kansas
Riley
Cretaceous

ABSTRACT

Dating kimberlite intrusive rocks by radiogenic isotope geochronology often is a difficult task, complicated by both the lack of dateable minerals within kimberlite as well as significant sample alteration that can degrade samples and alter parent–daughter ratios. This study presents a new geochronologic tool for timing the emplacement of kimberlites using the (U–Th)/He system to date the cooling of common kimberlite phenocrystic and xenocrystic minerals. To demonstrate the use of this technique, new apatite, titanite, zircon, magnetite and garnet (U–Th)/He ages constrain the timing of emplacement for the Stockdale, Tuttle, Baldwin Creek, Bala, and Leonardville kimberlite pipes, located in Riley County, Kansas. Zircon from the Tuttle pipe and titanite from the Stockdale pipe yield (U–Th)/He ages of 108.6±9.6 Ma and 106.4±3.1 Ma, respectively. These data are consistent with new Tuttle kimberlite Rb–Sr analyses of phlogopite megacrysts that give a five point isochron age of 106.6±1.0 Ma. Similarly, an apatite (U–Th)/He age of 85.3±2.3 Ma from the Baldwin Creek kimberlite is in agreement with a Rb–Sr phlogopite age of 88.4±2.7 Ma. These dates demonstrate that (U–Th)/He thermochronometry provides reliable timing constraints on the cooling of common kimberlite xenocrystic phases, thereby timing kimberlite emplacement. In addition to the use of more commonly used apatite and zircon (U–Th)/He thermochronometers, we produced reliable emplacement ages of 103.0±7.5 Ma for the Bala kimberlite using (U–Th)/He dating of phenocrystic magnetite and an age of 98.8±8.9 Ma for the Tuttle kimberlite using (U–Th)/He dating of megacrystic garnet. In contrast, kimberlitic apatite (U–Th)/He ages from the Stockdale, Bala, Tuttle, and Leonardville kimberlites yield ages ranging from 67.3±4.4 Ma to 64.3±5.6 Ma, suggesting a local, possibly hydrothermal reheating event resulting in resetting of the apatite (U–Th)/He clock in latest Cretaceous to earliest Tertiary time. Additional (U–Th)/He analyses of apatite from nearby sandstone and basement rocks suggest regional cooling below ~70 °C at ~165 Ma. These (U–Th)/He and Rb–Sr age data imply that the kimberlites were emplaced over a period of time from ~85–110 Ma with several pipes subjected to local reheating at ~65 Ma.

1. Introduction

Besides their economic importance as host rocks for diamonds, kimberlites have significantly contributed to the petrologic and geochemical understanding of the mantle. These potassic–ultramafic intrusive rocks are thought to be associated with explosive CO_2 mantle degassing, causing rapid ascent of kimberlitic magma and the consequent delivery of mantle and crustal xenoliths to Earth's surface. Accurate determination of the age and duration of kimberlite events can provide information on the genesis of these magmas and their relation to the geodynamic setting of the mantle and overlying crustal sections.

Compilations of North American kimberlite temporal and location data show two large continental-scale corridors of kimberlite magmatism (Meyer, 1976; Crough et al., 1980; Heaman et al., 2003, 2004). First, and most notable, is a N–S trending, corridor extending from Somerset Island, Canada, south to Kansas with kimberlite eruptions occurring over a ~30 Ma period during the Cretaceous (Heaman et al., 2004). The origin of this North American Cretaceous kimberlite corridor is unclear and both subduction and extensional tectonic settings have been suggested to explain this N–S trend (McCandless, 1999; Heaman et al., 2004). A second NW–SE trending corridor stretching from Washington State to Bermuda has been suggested to be the volcanic record of the Bermuda hotspot as it passed underneath North America (Crough et al., 1980; Morgan, 1983; Cox and Van Arsdale, 1997). Due to a lack of timing constraints, the relation between the evolution of North American kimberlites and their tectonic setting is not well understood. In addition to developing new applications for (U–Th)/He dating, a major motivation behind this study is to investigate the timing of Kansas kimberlite emplacement. A better temporal understanding of events in the mid-continent will allow us to evaluate possible tectonic settings and sources responsible for the kimberlites in Kansas and their relation to other kimberlites in North America.

* Corresponding author.
E-mail address: terrence@mit.edu (T.J. Blackburn).

0012-821X/$ – see front matter © 2008 Elsevier B.V. All rights reserved.
doi:10.1016/j.epsl.2008.08.006

This study will demonstrate that (U–Th)/He dating of kimberlitic apatite, titanite, zircon, magnetite and garnet can yield reliable ages on the emplacement of kimberlite magmas into the upper crust. The variability in kimberlite mineralogy combined with sample serpentinization and weathering often makes kimberlite radiometric dating difficult to impossible. If kimberlite phenocrystic mineralogy is devoid of dateable phases such as perovskite and phlogopite, (U–Th)/He dating of apatite, zircon, titanite, magnetite and garnet, common xenocrystic and phenocrystic phases, may be the best option for constraining the age of eruption. These minerals have relatively low helium closure temperatures (Reiners and Farley, 1999; Farley, 2000; Reiners et al., 2004). As a result, xenocrystic grains should have their helium clocks reset upon entrainment within the kimberlite magma, only to start their radiogenic helium clock upon rapid cooling within the kimberlite pipe. Helium closure temperatures of zircon and titanite are high enough to prevent subsequent resetting of their radiogenic clock, preserving the parent to daughter ratio from the time of kimberlite emplacement. The low closure temperature of the apatite (U–Th)/He system (70 °C) may allow this thermochronometer to become reset during geologic events subsequent to kimberlite emplacement. Significant crustal erosion, for example, would exhume kimberlitic apatite that may not have cooled below apatite helium closure during kimberlite emplacement. If prior to denudation these apatite grains were kept above 70 °C, the (U–Th)/He age will yield an age younger than that of kimberlite emplacement. Despite the possible complications using this low temperature chronometer, the subsequent thermal history of the kimberlite can be evaluated by both geologic constraints on erosion and (U–Th)/He dating of apatite from the surrounding country rock. If erosion or fluids have affected the kimberlitic apatite (U–Th)/He clock, the geologic mechanism should also reset the apatite (U–Th)/He clock in the surrounding rocks.

1.1. Geologic setting and existing age information for Kansas kimberlites

The kimberlites of Riley and Marshall Counties are located just east of the mid-continent rift system in north-eastern Kansas (Fig. 1) and intrude Permian age limestone and shale of the Chase group (Brookins, 1970; Brookins and Naeser, 1971; Mansker et al., 1987; Berendson and Weis, 2001). Five of the twelve Kansas kimberlites crop out at the surface and two additional kimberlites create surface expressions (Brookins, 1969, 1970; Brookins and Naeser, 1971; Mansker et al., 1987). The majority of the Kansas kimberlites, however, are obscured by glacial till and colluvium, though their presence has been confirmed by drill core (Brookins, 1970; Mansker et al., 1987). In the Winkler kimberlite, the upper tuffaceous material of this crater facies diatreme has been preserved underneath several feet of glacial material. The preservation of this sub-aerial kimberlite rock indicates minimal erosion since eruption (Brookins, 1970; Mansker et al., 1987).

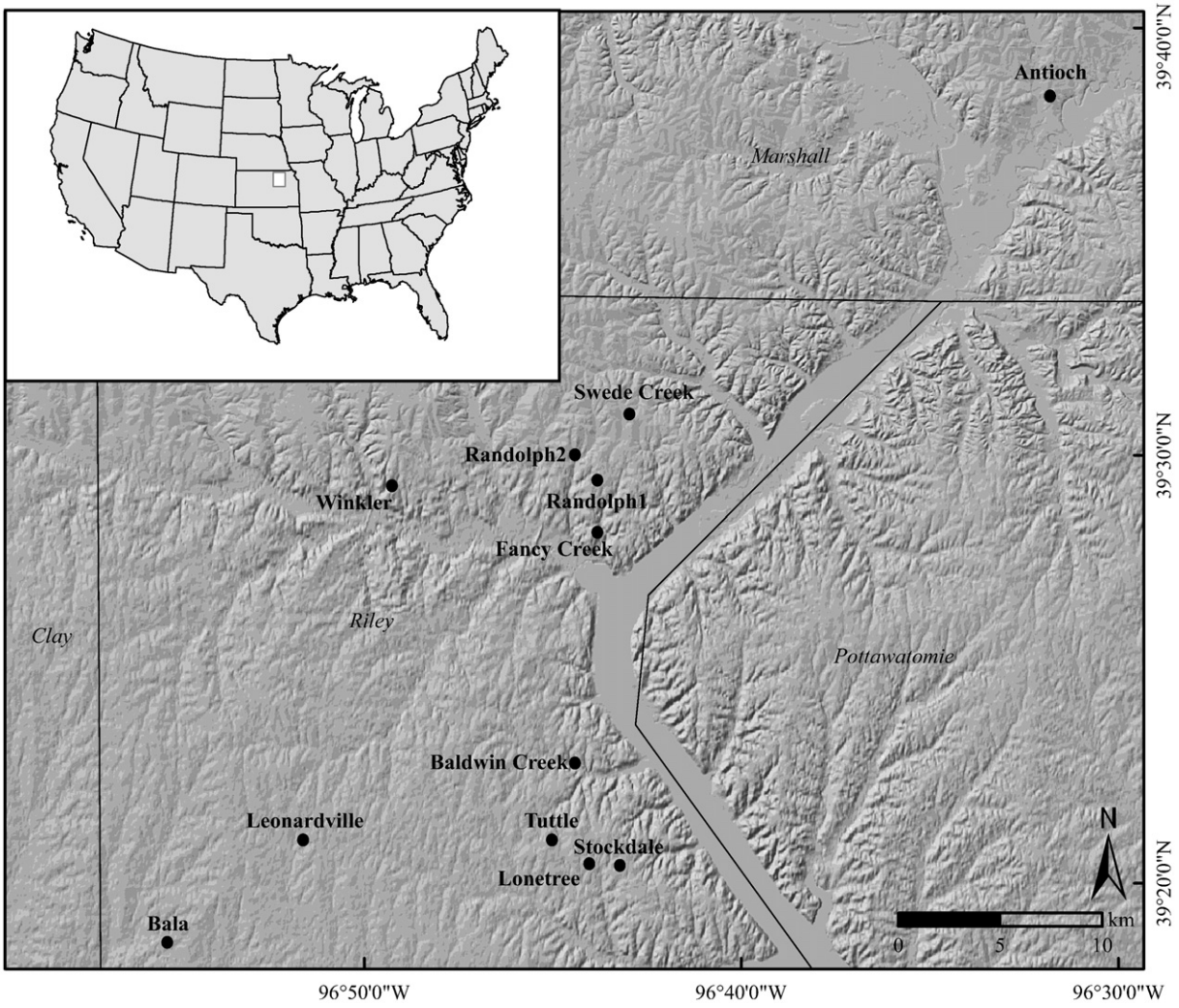

Fig. 1. Locations of all 12 kimberlites in Riley and Marshall Counties Kansas, USA. Only five kimberlites, Stockdale, Randolph 1 and 2, Fancy Creek, and Bala crop out at the surface. All five of these pipes were sampled plus 3 additional kimberlite pipes; Tuttle, Leonardville and Baldwin Creek, were sampled from drill core.

Consequently, the other eleven kimberlites as well as the surrounding region have also experienced minimal erosion. Preservation of the Cretaceous Palmetto Formation (basal Dakota Formation) in western Riley County supports the proposition that the area has had minimal material removed (Smith and Archer, 1995).

All five exposed kimberlites were sampled for this study and an additional three kimberlites were sampled from drill core (Mansker et al., 1987; Berendson and Weis, 2001). The most common kimberlite facies in Kansas is the brecciated diatreme facies. This rock is representative of the upper portions of a kimberlite diatreme, made up mostly of country rock fragments and large phenocrysts within a kimberlitic matrix. By far the most common xenoliths in the Kansas crater and diatreme pipes are limestone and shales from the surrounding Permian strata. Mantle, upper and lower crustal xenoliths are found at the better outcrops, though mantle and lower crustal samples are typically heavily weathered and small. Granitic xenoliths from the upper crustal basement are rare, but can be as large as 10 cm in diameter. These rare samples provide an excellent source of dateable materials for (U–Th)/He geochronology. The less common kimberlite facies in Kansas is the hypabyssal variety, in which the rock is mostly kimberlitic matrix with small phenocrysts and few xenoliths. In both kimberlite facies, olivine is the dominant phenocryst, but is usually completely serpentinized. Ilmenite, magnetite, calcite, pyroxenes, pyrope, and phlogopite are all common. An additional feature in nearly all Kansas kimberlites is the presence of calcite veins that occasionally contain magnetite coexisting within the center of the calcite vein. (Cullers, 1982). The veins cross-cut kimberlite flow fabric as well as xenoliths within the kimberlites. An in depth discussion of the geologic setting, mineralogy, petrology and major and trace element chemistry of the Kansas kimberlites has been provided by previous studies (Brookins, 1969, 1970; Brookins and Naeser, 1971; Cullers, 1982; Mansker et al., 1987; Berendson and Weis, 2001).

Previous attempts to date the Kansas kimberlites used K–Ar dating of phlogopite and produced variable ages for the Stockdale kimberlite between 204±20 Ma to 380±40 Ma (Brookins, 1970; Brookins and Naeser, 1971). These ages, which exceed the age of the sedimentary country rocks intruded by the kimberlites, can likely be attributed to excess ^{40}Ar in kimberlitic micas, a problem that has been well documented in other kimberlite dating studies (Allsopp et al., 1986). Another effort to date the kimberlites attempted to time the cooling of biotite from a granitic xenolith, and yielded a younger K–Ar age of 112±6 Ma (Brookins and Naeser, 1971).

In addition to K–Ar dating, this previous study dated two Kansas kimberlites by apatite fission track methods using apatite separated from granitic xenoliths (Brookins and Naeser, 1971). Apatite fission track ages of 123±12 Ma and 115±12 Ma from the Stockdale and Bala kimberlites, respectively, were interpreted to indicate the timing of kimberlite cooling during rapid emplacement (Brookins and Naeser, 1971). These apatite fission track ages appear to be in reasonable agreement with the singular xenolith K–Ar age described above, however the fission track methods employed did not include measurement of track lengths and hence allow no estimate of post-emplacement annealing. The same apatite mineral separates used for this fission track study were lent to our study and dated by apatite (U–Th)/He methods.

2. Methods

2.1. Sample description

For this study, five of the twelve kimberlites from Riley and Marshall Counties were dated by (U–Th)/He and/or Rb–Sr techniques. The remaining eight kimberlites were unsuitable for thermochronometric dating due to inaccessible outcrops, inappropriate mineralogy, or extreme alteration. Kimberlite rock samples were separated for apatite, titanite, zircon and phlogopite using standard rock crushing, heavy liquid, magnetic separation and hand picking techniques.

2.1.1. Tuttle kimberlite

The Tuttle kimberlite was sampled from drill core (operator: Kansas Geological Survey, core ID#: kimberlite 75-1) at depths of 30 and 90 meters. Common phases in this diatreme facies pipe include large megacrystic pyrope garnet, ilmenite, clinopyroxene, and phlogopite. Accessory phases include apatite, rutile, and at particular depths, titanite (30 m) and zircon (90 m). The Tuttle kimberlite is not exposed at the surface, which limits the potential of finding the rare and small crustal and mantle xenoliths that are characteristic of other crater and diatreme facies Kansas kimberlites.

2.1.2. Stockdale kimberlite

The Stockdale kimberlite is the best exposed Kansas kimberlite, providing the opportunity to collect mantle, lower and middle crustal xenoliths as well as larger quantities of kimberlite. This kimberlite is a highly brecciated crater facies pipe, consisting of up to ~50% upper crustal limestone and shale xenoliths. Common megacrystic phases include pyrope, ilmenite, and phlogopite that are usually highly fractured and infiltrated by kimberlite magma, making age dating of these megacrystic phases difficult for this particular pipe. Common accessory phases in the Stockdale kimberlite include magnetite, and clinopyroxene. Large granitic xenoliths sampled from within the kimberlite have provided us with dateable materials that we assume were entrained and then cooled upon kimberlite emplacement.

2.1.3. Baldwin Creek kimberlite

The Baldwin Creek kimberlite is a brecciated diatreme facies kimberlite that is not exposed at the surface. Drill core (operator: Kansas Geological Survey) from Baldwin Creek was collected at the depth of 90 m. Large megacrystic phases include pyrope, ilmenite, and phlogopite. Accessory phases include rutile, clinopyroxene, apatite, and zircon. All phases except the heavily metamict zircon are likely of kimberlitic origin.

2.1.4. Bala kimberlite

The Bala kimberlite is the only hypabyssal facies pipe on which we obtained age data. This fine-grained kimberlite is made of mostly kimberlite matrix and yielded no dateable phenocrystic phases. Accessory phases include magnetite, calcite and pyrope. Rare granitic xenoliths have been found from which apatite was originally separated for the aforementioned fission track study (Brookins and Naeser, 1971). Calcite veins are extremely abundant (occasionally containing calcite and magnetite), may be as wide as 10 cm and cross cut the kimberlite matrix and its flow fabric (Cullers, 1982).

2.1.5. Leonardville kimberlite

The Leonardville kimberlite is a diatreme facies kimberlite in the vicinity of the Tuttle and Stockdale pipes. Samples were collected from drill core (Operator: Kansas Department of Transportation, Well ID: 36–101 K-4044-011.14) at several depths <30 m. Common phenocrystic phases include clinopyroxene, pyrope, and lesser phlogopite, ilmenite and apatite. The apatite grains dated by (U–Th)/He methods were typically large, rounded, frosted and highly pitted suggesting that the mineral is either detrital in origin or possibly abraded during kimberlite ascent.

2.2. (U–Th)/He geochronology and methodology

2.2.1. Apatite, zircon and titanite (U–Th)/He methodology

(U–Th)/He dating of apatite, zircon and titanite have been successfully applied as reliable low temperature thermochronometers (Zeitler et al., 1987; Wolf et al., 1998; Reiners and Farley, 1999; House et al., 2000; Farley, 2000, 2002; Reiners et al., 2002, 2004; Stockli and

Farley, 2004; Reiners, 2005). The radiogenic daughter in this system, ^{4}He is produced by the α-decays of ^{238}U, ^{235}U, ^{232}Th and ^{147}Sm. The degree to which He is retained within intracrystalline sites can be determined by step-heating fractional loss diffusion experiments. Results from diffusion experiments should yield an Arrhenius relationship from which a minerals' activation energy (E_a), and diffusion coefficient (D_0) can be derived. Using Dodson's (1972) equation, the kinetic parameters for a mineral can then be used to calculate a helium closure temperature (T_C) (Dodson, 1972). The Helium T_C for a mineral has become an important concept allowing us to understand the different temperatures at which a mineral's (U–Th)/He clock starts. The He T_C of apatite, titanite and zircon will play in an important role in the interpretation of our kimberlitic multi-phase (U–Th)/He data. Apatite has the lowest closure temperature of ~70 °C (Farley, 2000). Zircon and titanite have higher closure temperatures of ~180 °C and 200 °C respectively (Reiners and Farley, 1999; Reiners et al., 2002, 2004).

In this study, apatite (U–Th)/He analysis were conducted following procedures similar to those in House et al. (2000) and Farley and Stockli (2002). Similarly, titanite (U–Th)/He analysis followed procedures by Stockli and Farley (2004), and Reiners and Farley (1999). Lastly, zircon (U–Th)/He analyses followed procedures by Reiners et al. (2002, 2004). Apatite and zircon (U–Th)/He ages were corrected for α-ejection using the F_T ejection correction method (Farley, 2002; Farley et al., 1996). The use of F_T correction methods relies on the assumption that parent elements, U and Th are homogenously distributed within the analyzed crystal. Two procedures were used for titanite α-ejection correction. The first technique takes advantage of titanite's typically large size and its tendency to fracture during rock crushing. Following procedures used by Stockli and Farley (2004) and Reiners and Farley (1999) the core of titanite grains are hand picked for analysis, and are interpreted to be free of grain edges that experienced α-ejection. A second batch of titanite grains from the Stockdale kimberlite were air abraded using methods similar to Krogh (1982). This additional abrasion step should ensure the removal of any additional crystal domains that may have experienced α-ejection. Sample heating for this study used a 20W Nd:YAG laser followed by ^{4}He measurement by isotope dilution, cryogenic purification, and measurement by quadropole mass spectrometry. For a more detailed discussion of laser heating and ^{4}He measurements see House et al. (2000) and Tagami et al. (2003). Measurements of U–Th concentration were carried out by a VG Plasmaquad-2 ICP-MS.

2.2.2. Magnetite and garnet (U–Th)/He geochronology

In addition to the more commonly used apatite and zircon He dating techniques, we attempted to time the cooling of a large (~0.3 cm wide) magnetite and calcite vein that intrudes the Bala kimberlite and a large 1 cm diameter garnet megacryst from the Tuttle kimberlite. To successfully date both magnetite and garnet using the (U–Th)/He technique requires the consideration of possible He contribution from the α-decay of ^{147}Sm. Samarium concentrations in these magnetite and garnet samples are commonly considerable (1–3 ppm) and coupled with low U–Th concentrations (U: 10 ppb–2 ppm; Th: 0–10 ppb) can make a ~5–20% difference in the calculated helium age for these samples. Low parent nuclide concentrations in these samples required sample sizes to be greatly increased. These larger sample sizes bring parent and daughter amounts within the instrumentation detection limits but consequently add large quantities of major elements that may inhibit U, Th and Sm measurements by ICP-MS. All large magnetite and garnet samples underwent a two-step column chemistry procedure to purify U, Th and Sm solutions. Detailed laboratory procedures are further described in Blackburn et al. (2007). Developing any mineral phase as a new (U–Th)/He chronometer requires users to demonstrate independence between a minerals effective U concentration ([U]+0.2*[Th]) and (U–Th)/He age (Fig. 2). Independence between these two parameters suggests that the He budget for a mineral phase is not controlled by He implantation from U and Th rich neighbouring crystals or inclusions. Fig. 2 contains no noticeable trends between (U–Th)/He age and effective U concentration suggesting the (U–Th)/He age calculated from these phases is unaffected by the amount of U and further signifying that all contributed He came from intracrystalline U and Th.

2.3. Rb–Sr phlogopite dating methodology

To evaluate the accuracy of our kimberlite (U–Th)/He ages, we attempted to obtain independent age constraints for kimberlite emplacement using methods with documented success in dating kimberlite eruptions. Single grain Rb–Sr analyses of kimberlitic phlogopite in several instances (Allsopp and Barrett, 1975; Allsopp et al., 1986; Brown et al., 1989) have produced isochron ages that are geologically reasonable and have low errors (<5% age variation). The cogenetic phlogopite often has widely different Rb/Sr ratios producing significant spread in the constructed isochron and thereby increasing precision of the resulting isochron age.

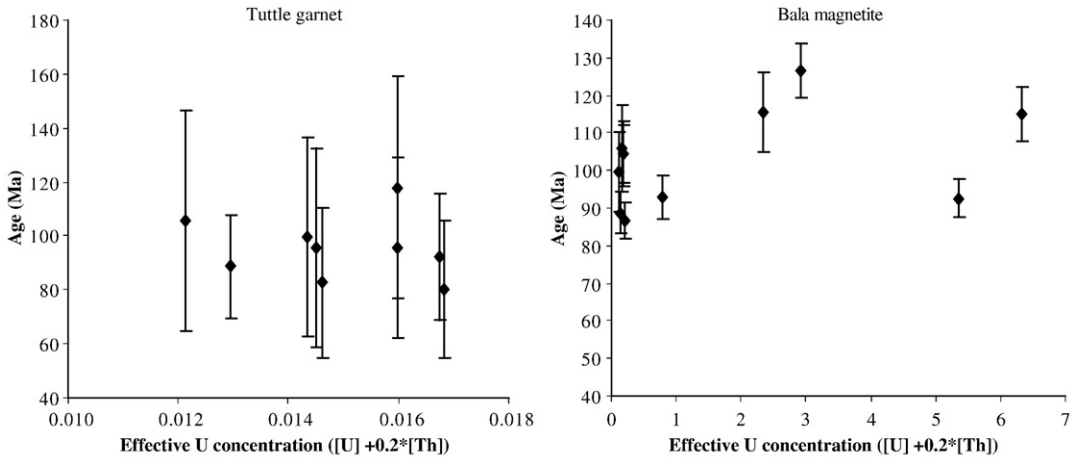

Fig. 2. Plot of effective U concentration ([U]+0.2*[Th]) vs. determined (U–Th)/He age for both magnetite and garnet kimberlite data. Developing magnetite and garnet as (U–Th)/He chronometers requires users to show that the He budget for these phases and thus the (U–Th)/He age is not controlled by He implantation from U and Th rich neighbouring crystals or inclusions. No noticeable trends in this data suggests that the (U–Th)/He age in these phases is unaffected by the amount of U further suggesting that all contributed He came from intercrystalline U and Th.

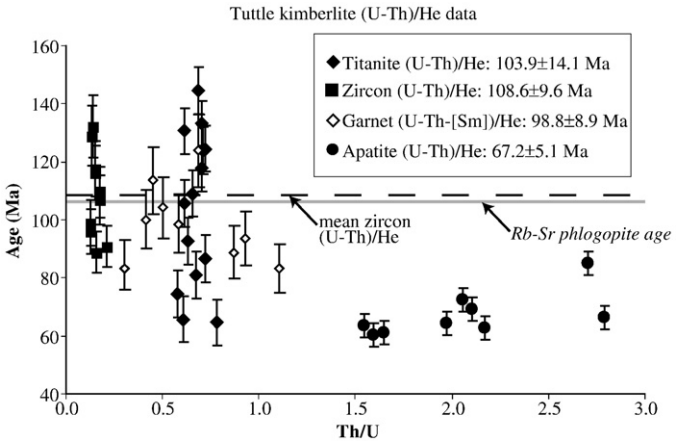

Fig. 3. Plot of zircon, titanite and apatite (U–Th)/He ages from the Tuttle kimberlite. Rb–Sr phlogopite age and errors in grey for comparison (Fig. 4a). Zircon (U–Th)/He analyses yielded the most reliable (U–Th)/He kimberlite eruption age for this pipe. The zircon (U–Th)/He age of 108.6±9.6 Ma (dashed line) is within error of the Rb–Sr isochron date. Gray line marks Rb–Sr age and extent of error. Several titanite grains and all apatite have seemingly been affected by a thermal event subsequent to kimberlite emplacement. A mean apatite (U–Th)/He age for the Tuttle kimberlite of 67.2±5.1 Ma, suggests a thermal pulse in the latest Cretaceous, approximately 40 million yr after the emplacement of this kimberlite.

The isotopic similarity of large megacrystic phlogopite, clinopyroxene, garnet and ilmenite demonstrate that these phases are likely to have crystallized simultaneously, in the earliest stages of a kimberlite magma (Nowell et al., 2004). The cogenetic nature of these minerals allows them to be employed as additional data points on a Rb–Sr isochron. The mineral clinopyroxene incorporates large amounts of initial Sr (~100 ppm) and minute amounts of initial Rb (~0.45 ppm). The extremely low parent to daughter ratio in clinopyroxene provides a constraint of the initial $^{87}Sr/^{86}Sr$ for kimberlite magma and its phlogopite, thereby improving the Rb–Sr isochron and resulting date.

Despite the common presence of phlogopite in crater and diatreme facies kimberlites, only two of the sampled pipes (Tuttle, and Baldwin Creek) contained phlogopite megacrysts with the minimal amounts of alteration suitable for analysis. Backscatter electron imaging of phlogopite from the Tuttle kimberlite revealed slight chloritization of the crystal edges. In addition to hand picking fresh samples, altered sample edges were cut away to remove areas that may have experienced parent/daughter fractionation. Each analyzed phlogopite was leached and ultra-sonicated in 2.5 N HCL for 10 min to remove surficial and interlayer strontium contamination from the kimberlite magma and/or subsequent fluids. Leaching samples ensures that measured $^{87}Sr/^{86}Sr$ ratios are from the radiogenic ingrowth within the mica (Brown et al., 1989). After leaching, samples were cleaned in water, dried and spiked with Rb and Sr tracers. Phlogopite grains were

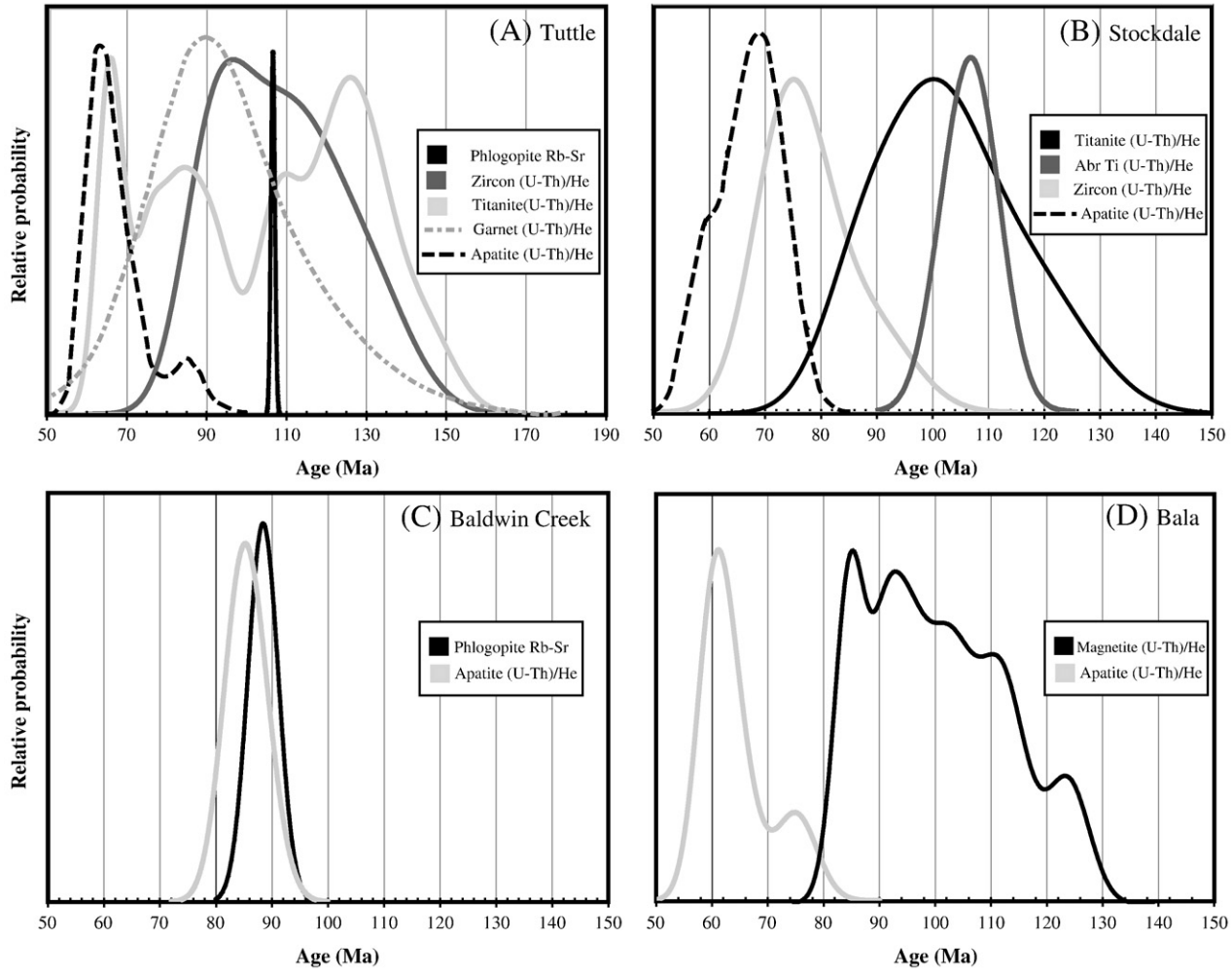

Fig. 4. Probability density plot of geochronologic data from each pipe. The obvious bimodal distribution of ages in most pipes suggest kimberlite emplacement at ~100 Ma followed by a thermal pulse at ~65 Ma. In one documented case, the Baldwin Creek kimberlite was emplaced at ~85 Ma and was left unaffected by the late Cretaceous thermal pulse. The highly variable mineralogy between kimberlites prevents successful dating with one geochronometer. Zircon data from the Tuttle pipe, abraded titanite data from the Stockdale pipe, apatite data from Baldwin Creek pipe and magnetite data from the Bala pipe are the best examples from this study for kimberlite (U–Th)/He geochronology.

dissolved in a typical 2 step acid treatment of HF+HNO_3 followed by HCl. Samples were heated on a hot plate for ~1 day for each acidification step. After dissolution, samples were chemically purified using Sr-spec columns. Purified Sr separates were analyzed by thermal ionization mass spectrometry (TIMS) using the Finnigan Triton at The Department of Terrestrial Magnetism (DTM). A Rb fraction was taken from the rinse or wash steps of the Sr column chemistry then dried and treated with a wash of hydrofluoric acid. The HF was dried down and then brought up in pure H_2O, which was extracted from undissolved solids with a pipette for Rb analysis. This fluorination step rapidly isolates Rb for removal, leaving behind a great deal of the remaining major elements. The Rb analyses were conducted first using the Finnigan Triton TIMS at DTM (TUPHL1-5, TUCPX-1). The remaining sample Rb analyses (TUPHL6-10, BCPHL1-5) were performed on the P54 sector multi-collector ICP-MS also at DTM. Rb concentration precision using the TIMS technique is estimated at ~2% and 1% using the ICP-MS with fractionation control being the main limiting factor in precision. The error of the blank correction, assuming a 50% variability in the blank was added to the isotope ratio uncertainties. A deteriorating polyethylene bottle used in the production of concentrated HCl contributed to a substantially elevated Sr blank (310 pg) for the second round of analyses reported here. Consequently, for the Tuttle locality, we restrict our discussion only to samples analyzed in the first analytical period (TUPHL 1-5, TUCPX-1) where the blank to sample ratio was much lower (blank 50 pg). For the Baldwin Creek samples (BCPHL) we apply correction for the large blank measured during this period to both the Sr concentration and isotopic composition. This has little effect on the concentration determinations, but does significantly increase the error on the Sr isotopic composition. For all these samples, the mass spectrometer run errors were below 0.00047 on $^{87}Sr/^{86}Sr$, in most cases well below 0.0001. All samples except for the clinopyroxene analyses, had mass spectrometer run errors well below the uncertainty added by the blank correction. Isochron ages and the corresponding age error were calculated using Isoplot (Ludwig, 2004).

3. Results

Because of the highly variable mineralogy in each pipe, there is no one kimberlite pipe dated by all of the methods described above. For each of the five dated kimberlites, the date for each geochronologic method is given along with an age comparison between these methods. The error assigned to each of the final apatite, titanite and zircon (U–Th)/He ages is the 2σ standard error (SDOM), calculated from the age data and the number of aliquots (N) per sample ($2*\mathrm{SDOM}=2*\sigma/\sqrt{N}$). The error assigned to each individual aliquot is based on the expected variation in ages demonstrated by previous (U–Th)/He studies; apatite (6%), zircon and titanite (8%). Because magnetite and garnet are not well established (U–Th)/He chronometers, the error assigned to each individual (U–Th)/He aliquot of magnetite and garnet has been propagated from the analytical error (U, Th, Sm, He measurement error). The final mean error weighted age for these magnetite and garnet (U–Th)/he analyses was calculated using Isoplot (Ludwig, 2004). All apatite, zircon, titanite, magnetite and garnet (U–Th)/He data are summarized in data repository 1 (DR1). All Rb–Sr phlogopite data are summarized in data repository 2 (DR2).

3.1. Tuttle kimberlite

Ten single grain zircon (U–Th)/He analyses of the Tuttle kimberlite yield a mean cooling age of 108.6±9.6 Ma (Fig. 3). Fourteen single grain titanite (U–Th)/He analyses from the Tuttle kimberlite produced a significant spread in ages. The great majority of these titanite ages are in good agreement with zircon (U–Th)/He data, although several ages are as young as 65 Ma (Fig. 3). A single, 1 cm diameter megacrystic garnet from the Tuttle kimberlite was isolated and crushed and dated by (U–Th-[Sm])/He methods. Despite extremely low parent nuclide concentrations, nine aliquots of over 1 mg each in size yield a mean age of 98.8±8.9 Ma. Lastly, several single to multiple grain apatite (U–Th)/He analyses from ~30 m depth within the Tuttle kimberlite give a mean cooling age of 67.2±5.1 Ma. Fig. 4A, a probability density diagram, plots the age data from each mineral separately illustrating the variability of (U–Th)/He age with mineralogy. The variability of ages with mineralogy suggests a complicated thermal history within the Tuttle pipe, one that we will explore further below.

In effort to evaluate these kimberlite (U–Th)/He ages, we dated the Tuttle kimberlite using Rb–Sr phlogopite/clinopyroxene geochronology. Rb–Sr analyses were performed on five individual phlogopite megacrysts and one clinopyroxene megacryst to construct a Rb–Sr isochron that regressed to an age of 106.6±1.0 Ma (MSWD=1.6)(Figs. 5 and 4A) excluding the outlier sample Tuphl-2. Excluding the clinopyroxene data from this line produces an overlapping age of 100.9±5.9 Ma.

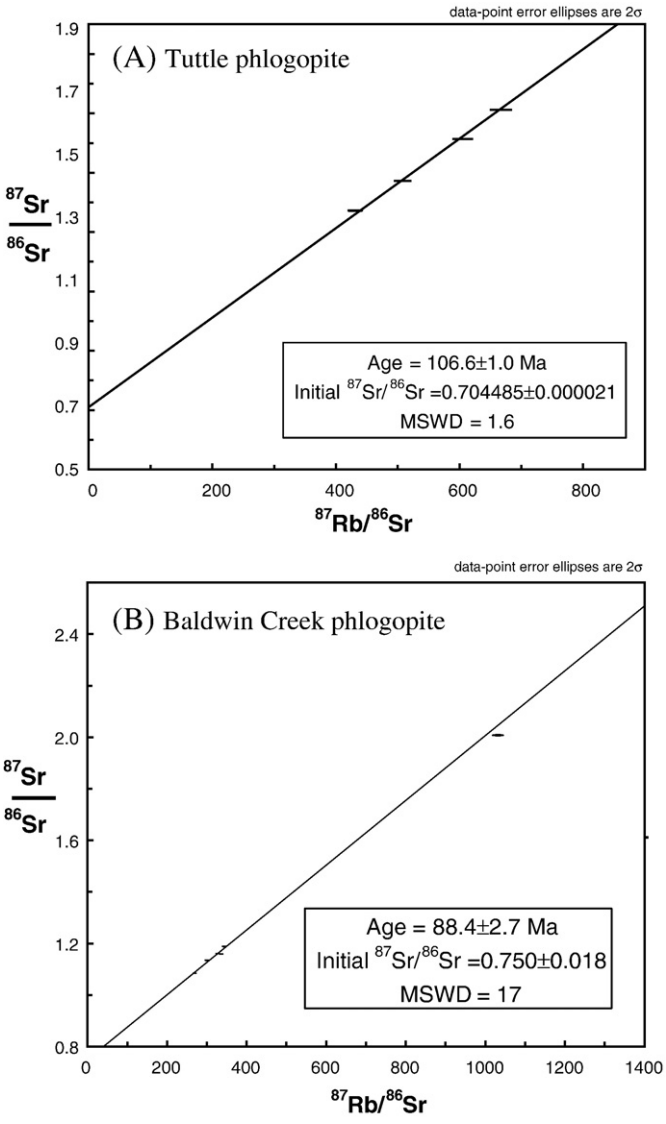

Fig. 5. Rb–Sr isochron ages for (A) Tuttle and (B) Baldwin Creek kimberlites. Kimberlites were dated by Rb–Sr techniques to provide a benchmark age to compare the experimental kimberlite (U–Th)/He ages. Dating phlogopite by Rb–Sr geochronology has for some time been utilized for kimberlite geochronology. The Tuttle Rb–Sr isochron is constructed of four single grain megacryst phlogopite and one clinopyroxene analyses. The Baldwin Creek isochron is made up of five phlogopite analyses.

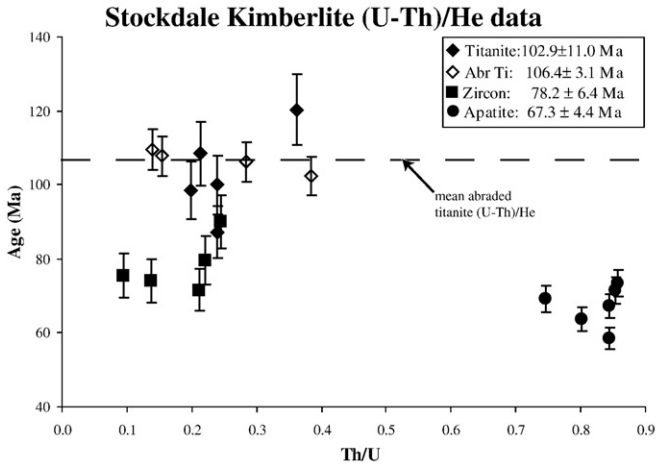

Fig. 6. Plot of xenocrystic zircon, titanite and apatite (U–Th)/He ages from granitic xenoliths found within the Stockdale kimberlite. (U–Th)/He analyses of abraded titanite produced the most reliable (U–Th)/He emplacement age for this kimberlite. A mean abraded titanite (U–Th)/He age of 106.4±3.1 Ma (dashed line) is not within error but in reasonable agreement with a previously determined fission track age of 123±12 Ma. Dated zircon grains were metamict and as a result were susceptible to helium loss during the late Cretaceous thermal event producing a partially reset age of 78.2±6.4 Ma. Apatite, with a He closure temperature even lower then metamict zircon is likely to be fully reset, recording a thermal event at 67.3±4.4 Ma.

3.2. Stockdale kimberlite

The Stockdale kimberlite is the best exposed kimberlite in northeastern Kansas, which, for this study, allowed us to find and extract a large mid to upper crustal granitic xenolith near the center of the diatreme. (U–Th)/He dating of these granitic mineral phases allows us to test the prediction that xenolithic phases within the kimberlite will have their helium clocks' completely reset by the magma, and allow us to date the emplacement of the pipe without consideration of inherited or initial daughter accumulation. Non-abraded titanite (U–Th)/He analysis from the Stockdale xenolith yield an age of 102.9±11.0 Ma, while abraded grains produced an age of 106.9±3.1 Ma (Figs. 6, 4B). Zircons from this xenolithic sample are metamict (brown, unclear in appearance) suggesting that the short holding time within the kimberlite magma is not sufficient to anneal radiogenic damage and the sample likely resided within the upper crust where damage from radiometric decay could accumulate. (U–Th)/He zircon analyses

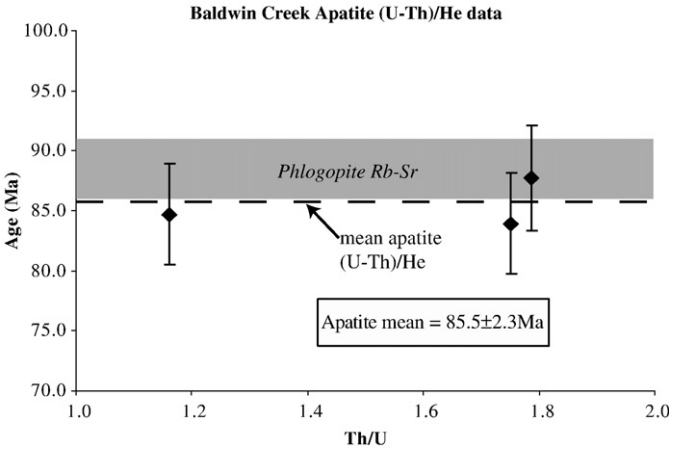

Fig. 7. Apatite (U–Th)/He age data for the Baldwin Creek kimberlite. The multi-grain (n=2–4) apatite (U–Th)/He age of 85.5±2.3 Ma (dashed line) is in excellent agreement with the Rb–Sr age shown in grey (Fig. 4b). In addition to a more recent eruption when compared to other dated Kansas kimberlites, Baldwin Creek kimberlitic apatite (U–Th)/He clock has not been reset by the Cretaceous thermal event that has produced an age of ~65 Ma in other kimberlite pipes.

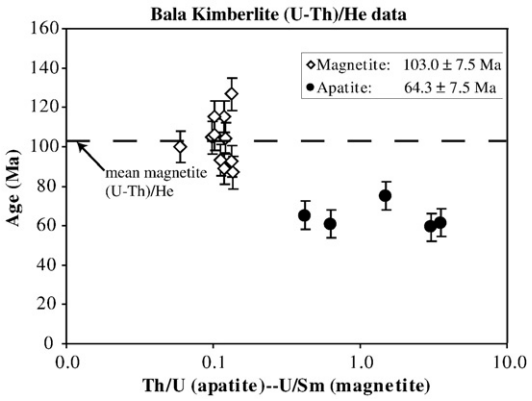

Fig. 8. Magnetite, and apatite (U–Th)/He age data from the Bala kimberlite. Preliminary efforts to date magnetite using the (U–Th)/He system has produced an age of 103.0±7.5 Ma (dashed line) that is in good agreement with a previously determined Bala kimberlite fission track age of 115±12 Ma. Apatite dated by the fission track study was re-dated by (U–Th)/He methods, yielding a much younger age of 64.3±7.5 Ma. Magnetite ages are plotted against U/Sm because of the low Th content in this particular magnetite.

from the same xenolith give a significantly younger age of 78.2±6.4 Ma (Figs. 6, 4B). Apatite (U–Th)/He ages from the Stockdale pipe were determined on grains from a different xenolith (sample: 1128a), collected for an earlier apatite fission track study (Brookins and Naeser, 1971). Despite a fission track age of 123±12 Ma, which is consistent with our Stockdale titanite results, our (U–Th)/He ages of the same apatite are considerably younger yielding an age of 67.3±4.4 Ma (Figs. 6, 4B).

3.3. Baldwin Creek kimberlite

The Baldwin Creek kimberlite contains large phenocrystic phlogopite as well as apatite of likely xenocrystic origin. Apatite quality in this sample was very suspect, yet despite the commonly abraded and pitted appearance our three aliquot multi-grain (n=2–4) analyses produced an age of 85.5±2.3 Ma (Figs. 7, and 4C). Rb–Sr analyses of six single grain phlogopites from the Baldwin Creek kimberlite yield an isochron age of 88.4±2.7 Ma (MSWD=17) (Figs. 5B and 7). This line is strongly controlled by the one phlogopite with very high Rb/Sr, but excluding this point from the line fitting changes the age only to 89±35 Ma with the uncertainty increasing dramatically because of the relatively small range in Rb/Sr of the phlogopites used to define this line.

3.4. Bala kimberlite

The hypabyssal facies Bala kimberlite when crushed and separated produced few, if any, dateable phases. Granitic apatite from sample Ka/R1

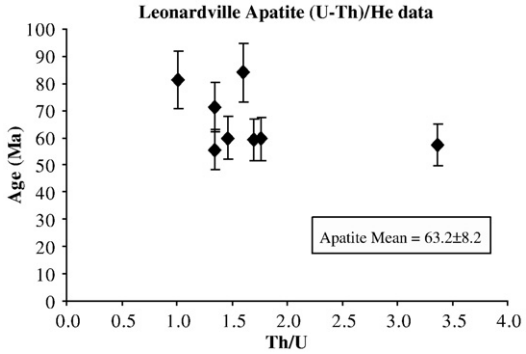

Fig. 9. Leonardville apatite (U–Th)/He data. A mean apatite (U–Th)/He age of 66.1±8.0 Ma suggests that some apatite is only partially reset by late Cretaceous re-heating. Several apatite ages are near as old as the moderate to high temperature geochronologic data collected from other kimberlites. No high temperature data was collected from this kimberlite.

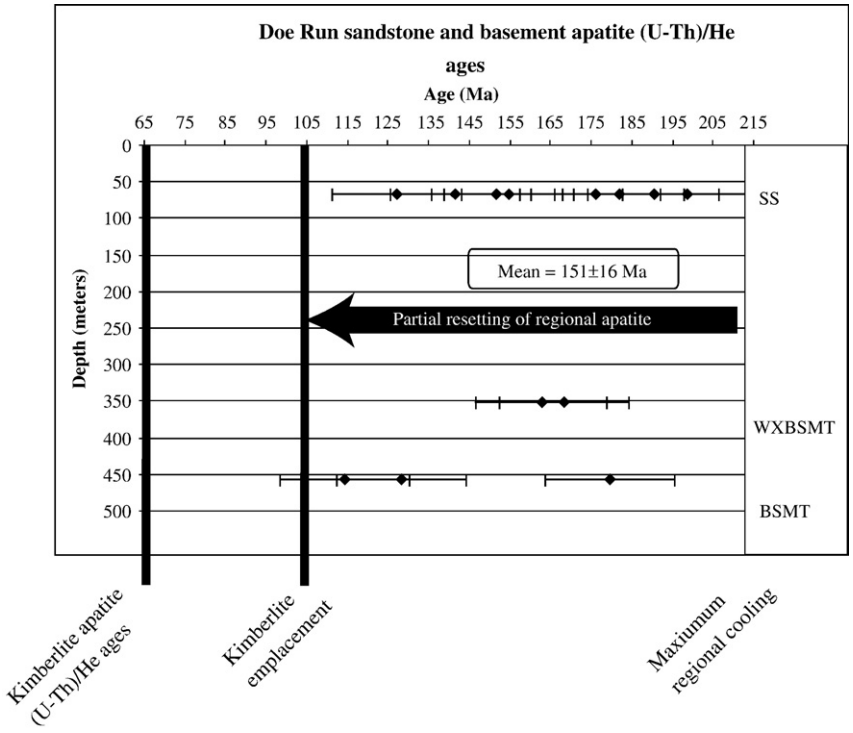

Fig. 10. Plot of apatite (U–Th)/He ages vs. drill core depth for country rock samples from nearby Marshall County, KS. The ages obtained by apatite (U–Th)/He analysis of the surrounding country rock show the "background" cooling age, and suggest a thermal history different than that of the typically younger kimberlite apatite (U–Th)/He ages. The sample at depth 66 m (SS) is course grain sandstone. Sample depth at 350 m (WXBSMNT) is from the narrow (20 cm) weathered basement horizon. Depth 457 m is the base of the drill core and (BSMT) is a sample of fresh syenite. A great range of dates were obtained reflecting a complicated thermal history in the region.

had previously been dated by apatite fission track and produced a seemingly reliable emplacement age of 115 ± 12 Ma (Brookins and Naeser, 1971). Similar to the Stockdale kimberlite, our single to multiple grain apatite (U–Th)/He analysis of this sample produced a significantly younger age of 64.3 ± 7.5 Ma (Figs. 8, 4D). A large magnetite and calcite vein from the Bala kimberlite was collected and used to attempt our first (U–Th)/He age dating of magnetite. This effort produced a reasonably reproducible magnetite (U–Th)/He age of 103.0 ± 7.5 Ma (Figs. 8, 4D) that is within error of the aforementioned fission track age.

3.5. Leonardville kimberlite

Near surface core samples from the Leonardville kimberlite yielded poor quality apatite. Despite pitted and abraded appearance we conducted several single to multiple grain analyses and produced a more dispersed age of 66.1 ± 8.0 Ma (Fig. 9). The two oldest apatite (U–Th)/He ages in the Leonardville data set approach the 85–88 Ma age determined here for the Baldwin Creek kimberlite.

3.6. Regional apatite (U–Th)/He cooling ages

Apatite bearing samples from a drill core of the nearby Permian age strata and Proterozoic basement, were crushed, separated and dated by apatite (U–Th)/He methods in order to evaluate if younger kimberlite apatite cooling ages could be produced by erosion or fluid migration. If the kimberlites have experienced a significant amount of erosion or heating during fluid migration resulting in apatite cooling after kimberlite emplacement, apatite from the surrounding country rocks should have had the same thermal history. This 457 m core (Operator: Doe Run, Well ID: DR-1, DR-1A) was sampled for apatite at depths of 66 m, 350 m and 457 m. The sample at 66 m is a course grained sandstone layer of the Permian Chase group. The sample at 350 m is the weathered syenite basement horizon, and the sample at 457 m is fresh basement syenite. Several single and multi-grain (n = 1–4) (U–Th)/He analysis were conducted on apatite mineral separates from all three samples. The two basement samples yield apatite (U–Th)/He ages varying between 115 and 165 Ma (Fig. 10). Apatite (U–Th)/He analysis of eight aliquots from the shallow sandstone produced a range of ages from 125 Ma to 195 Ma (Fig. 10).

4. Discussion

4.1. Kimberlite emplacement ~85–110 Ma

Phlogopite Rb–Sr analyses from the Tuttle kimberlite produced an isochron age of 106.6 ± 1.0 Ma (Fig. 5A). Tuttle zircon (U–Th)/He ages support the Rb–Sr age, giving a mean age of 108.6 ± 9.6 Ma (Fig. 3). The good agreement of ages at ~107 Ma between these moderate to high temperature geochronometers indicate that the Tuttle kimberlite was emplaced at this time. Apatite (U–Th)/He produce ages for the Tuttle pipe that are inconsistent with kimberlite emplacement, indicating that this chronometer has been subsequently reset.

Ages produced by Rb–Sr dating of the Baldwin Creek are younger suggesting a more recent eruption at 88.4 ± 2.7 Ma (Fig. 5B). Baldwin Creek apatite (U–Th)/He ages, unlike all other kimberlitic apatite, are in excellent agreement with the Rb–Sr age for kimberlite emplacement. The agreement between the high temperature and low temperature radiogenic ages from Baldwin Creek shows that this kimberlite has been emplaced more recently than others and has not experienced a younger thermal event affecting the apatite (U–Th)/He system (Fig. 7, 4C). A Baldwin Creek eruption age younger than Tuttle, Stockdale and Bala kimberlites reveals a more complex history for the emplacement of these kimberlites in Kansas. Although variability in kimberlite emplacement ages is not uncommon (Allsopp et al., 1986), the geodynamic setting responsible for reoccurring kimberlite magmatism within a province over a significant amount of time (10–30 Ma) is poorly understood. This variability in ages within the Kansas kimberlite province adds a complexity to any geodynamic model and also

demonstrates the need for a more multi-faceted geochronological approach to constrain the complete temporal evolution of a kimberlite province.

Titanite (U–Th)/He analyses from the Stockdale kimberlite yield a reproducible age for kimberlite emplacement at 102.9±11.0 Ma (non-abraded) and 106.4±3.1 Ma (abraded) and are slightly younger than the previously determined fission track age of 123±12 Ma (Fig. 6 and 4B). These results suggest that the use of mechanical air-abrasion (Krogh, 1982) to remove possible α-ejection surfaces dramatically improves the reproducibility between individual analyses. The high variability in ages in un-abraded samples indicates that these titanite grains contained some domain that had experienced He loss due to α-ejection. Future studies using titanite (U–Th)/He dating as a volcanic geochronometer would likely find an improvement in age precision when using mechanical air-abrasion to ensure removal of ejection surfaces.

Age data from the Bala kimberlite are unique in that we used magnetite as a (U–Th)/He geochronometer. This first recent effort using magnetite (U–Th)/He age dating produced a reliable age for kimberlite emplacement of 103.0±7.5 Ma that agrees well with the previously determined apatite fission track age of 115±12 Ma (Fig. 8, 4D). The age agreement between the two geochronometers demonstrates that magnetite (U–Th)/He dating can provide accurate and reproducible ages for the eruption of a kimberlite. In the Kansas kimberlites, magnetite is a ubiquitous mineral that could be utilized further to place more complete age constrains on the kimberlites in the region.

4.2. Reheating at ~65 Ma

The majority of kimberlitic apatite (U–Th)/He ages are significantly younger than determined emplacement ages. The younger ages produced by this low temperature thermochronometer suggest subsequent reheating in the area near the Cretaceous–Tertiary boundary. The exception is the Baldwin Creek kimberlite, whose apatite ages agree with Rb–Sr results and was not reheated at 65 Ma. The other dated pipes (Tuttle, Stockdale, Bala, and Leonardville) were subjected to a thermal pulse that did reset the apatite (U–Th)/He radiogenic clocks. In addition, titanite from the Tuttle kimberlite, and zircon from the Stockdale kimberlite seem to be at least partially affected by this event. Although the majority of Tuttle titanite (U–Th)/He analyses show cooling at ~100 Ma, several grains yielded considerably younger ages, indicating that reheating at 65 Ma was hot enough to affect some titanite grains. The Stockdale zircon, derived from a granitic xenolith of shallow depths, were metamict and prone to helium loss at temperatures that are lower than ideal zircon helium closure.

Apatite (U–Th)/He analysis of nearby sandstones and basement were conducted to determine if regional apatite has experienced a similar thermal history as kimberlitic apatite. The two deeper basement samples yield apatite (U–Th)/He ages between 115 and 165 Ma suggesting regional cooling in the Late Jurassic to Early Cretaceous that may have been partially reset in some subsequent thermal event (Fig. 10). Apatite (U–Th)/He analysis of the sandstone at 66 m produced ages ranging from 125 Ma to 195 Ma suggesting a cooling history that may be complicated by both kimberlite emplacement into the region (partial helium clock resetting) and a detrital cooling history. From these data alone, the thermal history of the surrounding country rock is not entirely clear. We can however, conclude that: (1) preservation of both Cretaceous sediments in far eastern Riley county and the presence of sub-aerial crater facies kimberlite indicate that the area experienced minimal amounts of regional erosion (Section 1.1) (Brookins, 1970; Mansker et al., 1987; Smith and Archer, 1995), (2) regional apatite has not experienced the same intensity of re-heating that kimberlitic apatite has at 65 Ma, and (3) the country rock is likely to have initially cooled below 70 °C at ~165 Ma, and has experienced some re-heating from either kimberlite emplacement at ~85–100 Ma or during fluid migration at ~65 Ma.

Cretaceous fluid migrations and thermal pulses within the Mid-continent have been well documented. Fluid inclusion data indicate that diagenetic calcite in Mid-continent limestone (including rocks in Kansas) have been reheated during some post-depositional fluid migration event (Barker et al., 1992; Wojcik et al., 1994; Newell, 1997). U–Pb/Th–Pb age data for calcite samples associated with ore deposits in Oklahoma produced ages within error of our 65 Ma apatite ages (Coveney et al., 2000). The fluid migration event that produced metal ore in Oklahoma south of the kimberlites, may have reached particular kimberlites with sufficient heat to affect the apatite (and in some cases titanite and zircon) (U–Th)/He systems. Though the extent, nature and cause of this ~65 Ma thermal even remains unclear with the present data, the data does strongly suggest that local reheating within the mid-continent has occurred. This further suggests that low temperature thermochronology will be a useful tool for future studies working to understand heat transfer in stable cratonic interiors.

5. Conclusion

5.1. (U–Th)/He kimberlite geochronology

Low temperature thermochronology can produce ages for kimberlite emplacement, but the accuracy of this approach depends on which mineral is used, and the post-emplacement thermal history of the kimberlite. (U–Th)/He thermochronometers with higher closure temperatures such as titanite and zircon seem to be the best suited for dating kimberlite emplacement. In addition to these more commonly used thermochronometers, we have shown that magnetite can yield reliable ages for a kimberlite eruption and in the future may serve as an excellent mineral for kimberlite (U–Th)/He geochronology. The helium closure temperatures for these minerals fills a convenient thermal window that is high enough to prevent subsequent He loss from reheating, and low enough to become completely de-gassed within a kimberlitic magma of accumulated helium if a crystal is xenolithic.

The (U–Th)/He thermochronology of the Kansas kimberlites shows that minimal amounts of erosion have occurred since the kimberlites erupted (Brookins and Naeser, 1971; Mansker et al., 1987; Smith and Archer, 1995; Berendson and Weis, 2001). (U–Th)/He dating would not be successful in dating most South African kimberlites, where significant erosion (Hawthorne, 1975; Partridge, 1998) will have exhumed material that did not cool below helium closure until well after kimberlite emplacement, producing anomalously young (U–Th)/He ages.

Acknowledgements

We would like to thank T.J. Dewane, Chris Hager, Kit Tincher, and Nathan Winters for their input, helpful discussions and assistance in the lab. Thanks to both Chuck Naeser and Bob Goldstein for lending samples to this study. A special thanks to Doug Walker, Gwen Macpherson and Lisa Stockli for their helpful reviews. This manuscript benefited from constructive reviews from both an anonymous reviewer and editor. Funding for this project was provided by the Kansas Geological Foundation, GSA South Central Section, University of Kansas Dept. of Geology, and The Department of Terrestrial Magnetism at The Carnegie Institution in Washington.

Appendix A. Supplementary data

Supplementary data associated with this article can be found, in the online version, at doi:10.1016/j.epsl.2008.08.006.

References

Allsopp, H.L., Bristow, J.W., Smith, C.B., Brown, R., Gleadow, A.J.W., Kramers, J.D., Garvie, O.G., 1986, A summary of radiometric dating methods applicable to kimberlites and related rocks, (Eds.), 4th International Kimberlite Conference Perth W.A., 343–357.

Allsopp, J.L., Barrett, D.R., 1975. Rb–Sr age determinations on South African kimberlite pipes. Physical Chemistry of the Earth 9, 605–617.
Barker, C.E., Goldstein, R.H., Hatch, J.R., Walton, A.W., Wojcik, K.M., 1992. Burial history and thermal maturation of Pennsylvanian rocks, Cherokee Basin, Southeastern Kansas. Oklahoma Geological Survey Circular 93, 299–309.
Berendson, P., Weis, T., 2001. New kimberlite discoveries in Kansas: magnetic expression and structural setting. Transactions of the Kansas Academy of Science 104, 223–236.
Blackburn, T.J., Stockli, D.F., Walker, J.D., 2007. Magnetite (U–Th)/He dating and its application to the geochronology of intermediate to mafic volcanic rocks. Earth and Planetary Science Letters 259, 360–371.
Brookins, D.G., 1969. The significance of K–Ar dates on altered kimberlitic phlogopite from Riley County, Kansas. Journal of Geology 77, 102–107.
Brookins, D.G., 1970. Factors governing emplacement of Riley County, Kansas, kimberlites. Kansas Geological Survey Bulletin 199, 1–17.
Brookins, D.G., Naeser, C.W., 1971. Age of emplacement of Riley County, Kansas, kimberlites and a possible minimum age for the Dakota sandstone. Geological Society of America Bulletin 82, 1723–1725.
Brown, R.W., Allsopp, H.L., Bristow, J.W., Smith, C.B., 1989. Improved precision of Rb–Sr dating of kimberlitic micas: an assessment of a leaching technique. Chemical Geology 79, 125–136.
Coveney, R.M., Ragan, V.M., Brannon, J.C., 2000. Temporal benchmarks for modeling Phanerozoic flow of basinal brines and hyrdrocarbons in the southern Midcontinent based on radiometrically dated calcite. Geology 28, 795–798.
Cox, R.T., Van Arsdale, R.B., 1997. Hotspot origin of the Mississippi embayment and its possible impact on contemporary seismicity. Engineering Geology 46, 201–216.
Crough, T.S., Morgan, J.W., B.R., H., 1980. Kimberlites: their relation to mantle hotspots. Earth and Planetary Science Letters 50, 260–274.
Cullers, R.L., 1982. The trace element content and petrogenesis of kimberlites in Riley County, Kansas, U.S.A. American Mineralogist 67, 223–233.
Dodson, M.H., 1972. Closure temperature in cooling geochronological and petrological systems. Contributions to Mineralogy and Petrology 40, 259–274.
Farley, K.A., 2000. Helium diffusion from apatite: general behavior as illustrated by Durango fluorapatite. Journal of Geophysical Research 105, 2903–2914.
Farley, K.A., 2002. (U–Th)/He dating: techniques, calibrations, and applications. In: D., P., Ballentine, C.J., Wieler, R. (Eds.), Noble Gases in Geochemistry and Cosmochemistry. Reviews of Mineralogy, vol. 47, pp. 819–844.
Farley, K.A., Stockli, D.F., 2002. (U–Th)/He dating of phosphates: apatite, monazite, and xenotime. In: M., K., Rakovan, J., Hughes, J.M. (Eds.), Phosphates. Reviews in Mineralogy, vol. 47, pp. 559–578.
Farley, K.A., Wolf, R.A., Silver, L.T., 1996. The effects of long alpha-stopping distances on (U–Th)/he ages. Geochimica et Cosmochimica Acta 60, 4223–4229.
Hawthorne, J.B., 1975. Model of a kimberlite pipe. In: Ahrens, L.H., Dawson, J.B. (Eds.), Physics and Chemistry of the Earth, vol. 9, pp. 1–15.
Heaman, L.M., Kjarsgaard, B.A., Creaser, R.A., 2003. The timing of kimberlite magmatism in North America: implications for global kimberlite genesis and diamond exploration. Lithos 71, 153–184.
Heaman, L.M., Kjarsgaard, B.A., Creaser, R.A., 2004. The temporal evolution of North American kimberlites. Lithos 76, 377–397.
House, M.A., Farley, K.A., Stockli, D.F., 2000. Helium chronometry of apatite and titanite using Nd-YAG laser heating. Earth and Planetary Science Letters 183, 365–368.
Krogh, T.E., 1982. Improved accuracy of U–Pb zircon ages by the creation of more concordant systems using an air abrasion technique. Geochimica et Cosmochimica Acta 46, 637–649.
Ludwig, K.R., 2004. Isoplot/Ex rev 3.06 A Geochronological Toolkit for Microsoft Excel. Berkeley Geochronology Center.
Mansker, W.L., Richards, B.D., Cole, G.P., 1987. A note on newly discovered kimberlites in Riley County, Kansas. Geological Society of America Special Paper 215, 197–204.
McCandless, T.E., 1999. Kimberlites: mantle expressions of deep-seated subduction. In: Gurney, J.J., Gurney, J.L., Pacsoe, M.D., Richardson, S.H. (Eds.), Proceedings of the 7th International Kimberlite Conference, vol. 2, pp. 545–549.
Meyer, H.O.A., 1976. Kimberlites of the Continental United States: a review. Journal of Geology 84, 377–400.
Morgan, J.W., 1983. Hotspot tracks and the early rifting of the Atlantic. Tectonophysics 94, 123–139.
Newell, K.D., 1997. Comparison of maturation data and fluid-inclusion homogenization temperatures to simple thermal models; implications for thermal history and fluid flow in the Midcontinent. Bulletin- Kansas Geological Survey 240, 13–27.
Nowell, G.M., Pearson, D.G., Bell, D.R., Carlson, R.W., Smith, C.B., Kempton, P.D., Noble, S.R., 2004. Hf isotope systematics of kimberlites and their megacrysts: new constraints on their source regions. Journal of Petrology 45, 1583–1612.
Partridge, T.C., 1998. Of diamonds, dinosaurs and diastrophism: 150 million years of landscape evolution in southern Africa. South African Journal of Geology 101, 167–184.
Reiners, P.W., 2005. Zircon (U–Th)/He thermochronometry. In: Reiners, P.W., Ehlers, T.A. (Eds.), Low-temperature Thermochronology: Techniques, Interpretations, and Applications. Reviews in Mineralogy and Geochemistry, vol. 58, pp. 151–179.
Reiners, P.W., Farley, K.A., 1999. Helium diffusion and (U–Th)/He thermochronometry of titanite. Geochimica et Cosmochimica Acta 63, 3845–3859.
Reiners, P.W., Farley, K.A., Hickes, H.J., 2002. He diffusion and (U–Th)/He thermochronometry of zircon: initial results from Fish Canyon Tuff and Gold Butte, Nevada. Tectonophysics 349, 247–308.
Reiners, P.W., Spell, T.L., Nicolescu, S., Zanetti, K.A., 2004. Zircon (U–Th)/He thermochronometry: He diffusion and comparisons with 40Ar/39Ar dating. Geochimica et Cosmochimica Acta 68, 1857–1887.
Smith, B.D., and Archer, A.W., 1995, Geologic map, Riley County: Kansas Geological Survey,, in Survey, K.G.: Lawrence, KS.
Stockli, D.F., Farley, K.A., 2004. Empirical constraints on the titanite (U–Th)/He partial retention zone from the KTB drill hole. Chemical Geology 207, 223–236.
Tagami, T., Farley, K.A., Stockli, D.F., 2003. (U–Th)/He geochronology of zircon using Nd-YAG laser heating. Earth and Planetary Science Letters 207, 57–67.
Wojcik, K.M., Goldstein, R.H., Walton, A.W., 1994. History of diagenetic fluids in a distant foreland area, Middle and Upper Pennsylvanian, Cherokee basin, Kansas, USA: fluid inclusion evidence. Geochimica et Cosmochimica Acta 58, 1175–1191.
Wolf, R.A., Farley, K.A., Kass, D.M., 1998. Modeling of the temperature sensitivity of the apatite (U–Th)/He thermochronometer. Chemical Geology 148, 105–114.
Zeitler, P.K., Herczeg, A.L., McDougall, I., Honda, M., 1987. U–Th–He dating of apatite: a potential thermochronometer. Geochimica et Cosmochimica Acta 51, 2865–2868.